Eurasian Journal of Physics and Functional Materials

2018, 2(3), 251-258

Synthesis of boride-titanium coatings by magnetron sputtering of composite targetss

A.S. Larionov *, E.A. Zhakanbaeyev, A.L. Kozlovski, A.S. Dikov, S.B. Kislitsin, L.V. Chekushina

Institute of Nuclear Physics, Almaty, Kazakhstan

E-mail: larionov@inp.kz

DOI: **10.29317/ejpfm.2018020306**
Received: 04.09.2018

The paper presents the results of investigations of the structure and phase composition of titanium boride coatings deposited by magnetron sputtering from a target of a complex composition onto a steel substrate. The target for magnetron sputtering was obtained by sintering boron carbide and titanium powders. The structure and elemental composition of the coating were studied using X-ray diffractometry (XRD), scanning electron microscopy (SEM) and the energy-dispersive spectral (EDS). It was established that the coating structure is a mixture of Ti_2B_5 and TiB_{12} phases with the total boron content of ≈ 80 at %, which is 4 times higher than the boron concentration in the coatings obtained by plasma spraying of the B_4C powder. The use of magnetron sputtered coatings of titanium boride coatings as neutron-absorbing materials will allow to reduce the coating thickness in comparison with the coatings from boron carbide synthesized by plasma spraying methods.

Keywords: copper sulfide, thermal conductivity, thermoelectric materials, superionic conductors.

Introduction

The problems of safe handling of radioactive waste (RW) and spent nuclear fuel (SNF) are important for countries developing nuclear power [1]. The current volume of accumulated radioactive waste and forecasts forits growth make it necessary to move to a higher level of organization of the process of handling radioactive waste and SNF, i.e., transfer them to a safe state throughout the period of potential radiation hazard. In addition to gamma-emitting radionuclides, SNF

contains fissile materials (^{235}U, ^{239}Pu, ^{241}Pu, and others), sources of neutron radiation, which leads to the regeneration of part of the fuel and an increase in the overall activity. Radiation safety can be improved by reducing the number of neutrons. For this purpose, neutron-absorbing materials are used. Such materials are used in manufacturing of transport packaging containers and hexagonal casing pipes for compact storage in the storage pools and transportation of nuclear fuel.Such materials must not only be able to absorb neutrons, but must also have a large safety factor, high corrosion and radiation resistance. Their design should be convenient in manufacturing and handling, with a small weight and overall dimensions. In manufacturing of transport containers of a new generation for transportation and long-term compact storage of spent nuclear fuel and neutron sources, neutron-absorbing materials are used [2-4].

Modern requirements to the neutron-absorbing materials dictate an increase in the level of absorption. There is a tendency to use for this purpose protective coatings from powdered boron-containing composites. The disadvantage of such technologies is fragility and low strength of the coatings. It is possible to solve problem by synthesizing a monolithic coating. To date, several types of such coatings are known. These are SAM 2×5, Boraltm and Metamictm [5] coatings, containing about 15 at. % of boron, which at a thickness of the order of 1 mm makes it possible to weaken the neutron flux considerably. Such coatings are synthesized by plasma spraying of B_4C powder.

In this paper, it is proposed to synthesize a B-Ti neutron-absorbing coating by the magnetron sputtering. The principal difference between this method and the existing analogues is that the technology of magnetron sputtering can provide a high density of boron atoms in the coating. The fundamental difference is that the density depends not on the size of the powder granules and the distance between them (about 100 nanometers), but on the parameters (interatomic distance) of the lattice of the formed compound (several angstroms). Magnetron sputtered TiB_2 coatings were not previously considered as neutron-absorbing coatings, but were primarily used as hardening corrosion-resistant coatings in instrumentation technology [6-8]. Magnetron sputtering is technologically well-developed method, widely used for synthesis of various types of coatings: hardening, corrosion-resistant, heat-resistant and others. We used the magnetron sputtering technology to formfirm, corrosion-resistance neutron-absorbing coatings. The main difficulty in implementing this technology for boron-containing coatings is that boron is a dielectric and deposition of boron-containing coatings is a rather complex task.

Materials, research technique and technology of coating synthesis

The austenitic stainless steel 12X18H9T was used as the substrate for coating. The elemental composition, according to XRD analysis on the spectrometer S1 TITAN (Bruker AXS) and EDS analysis on the scanning electron microscope PHENOM XL (Phenom-World) is presented in Table 1. The steel surface was subjected to grinding (fine grinding, polishing), roughness is higher than Ra =

0.8 nm.

Table 1.
Elemental composition of steel 12X18H9T.

Element	Fe	Cr	Ni	C	Si	Mg	
at. %	71.46	16.88	8.74	4.23	1.38	0.49	
Element	In	Ru	Cu	Ti	Mo	V	W
at. %	0.43	0.38	0.26	0.14	0.04	«0.08	«0.08

As pure boron is a dielectric, boron carbide B_4C was used to fabricate the cathode target for the magnetron. To increase the electrical conductivity, titanium was added to the target. Thus, the magnetron target was a sintered mixture of B_4C and Ti powders with a mass ratio of 1:1. The production of a cathode target for a magnetron installation was carried out by hot pressing a mixture of B_4C and Ti powders in a vacuum at a pressure of $\sim$300 MPa and a temperature of $\sim$ 800 °C, with subsequent annealing at a temperature of 1250 °C. The specific surface area is $\sim$ 0.1 m^2/g. This configuration of the target makes it possible not only to increaseits electrical conductivity but also to shorten the time of coatingsynthesis.

Sputtering of the target was carried out on a magnetron installation VUP-5M (DC). A vacuum of $\sim 10^{-5}$ Pa was created in the working chamber, then a plasma-forming gas (Ar) was pressurized and its pressure was $\sim 2 \times 10^{-3}$ Pa. The magnetron was supplied with a voltage of 600 V, and a current of 70 A (power W $\sim$ 42 kW). The sprayed time was 30 minutes.

The composition of the obtained coating was studied by EDS method using a Hitachi TM 3030 scanning electron microscope. XRD analysis was carried out on a D8 ADVANCE ECO diffractometer (Bruker, Germany) using copper CuK α radiation. To identify the phases and to study the crystal structure, the software BrukerAXSDIFFRAC.EVAv. 4.2 and the international ICDD PDF-2 database were used. X-ray diffraction patterns were measured for the following parameters: Voltage - 40 kV, Current - 25 mA, 2θ = (48-82)^o, step 0.03^o, standing time at the point - 5 s, nickel solder was used as the absorber. Under these survey conditions, the penetration depth of X-rays into the material was not more than (8-10) μm. The film thickness was determined by the Rutherford backscattering spectrometry (RBS) on 1 MeV protons on the heavy ion accelerator UKP-2-1 (INP, Kazakhstan).

Results and Discussion

The main tasks during the experiment of magnetron synthesis of the coating with the B-Ti system were to establish the efficiency of using a cathode target of a complex composition and determine the growth rate of the film on the surface of the substrate. According to the RBS analysis, the thickness of the coating is 370 nm. The EDS analysis shows that the depth of penetration of electrons into the material is $\approx 1\,\mu m$, which exceeds the thickness of the resulting film. The obtained spectrum contains the data on the composition of coatings and substrates. To obtain a more precise ratio of elements in the coating, the analysis

was carried out on the areas with and without coating. For this purpose, the sample was placed at an angle of $\approx 45^{o}$ to the detector. This view provided an opportunity to observe the edge of the sample with a visible contrast between the substrate and the coating. Figure 1 shows the surface of the sample, indicating the points at which the analysis was carried out (a) and the distribution of Ti on the surface (b).

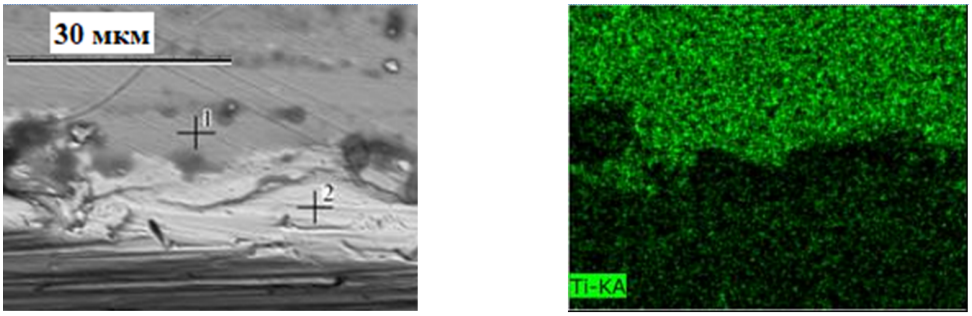

a b

Figure 1. Surface of the sample with B-Ti coating: a - location of the points of spectral analysis (1 – on the coated area, 2 – on the uncoated area); b – the map of Ti distribution on the surface.

The map of Ti distribution on the surface, by the difference in its content in the substrate material and in the coating, enables us to determine the boundary of this coating. Table 2 shows the elemental composition at points 1 and 2. Comparing the ratio of the elements in the volume of the material in the areas with and without coating, it can be concluded that $\approx 55\%$ of the spectrum at the point with the coating corresponds to the composition of the substrate. Due to the sputtering conditions, the coating cannot contain Fe, and the substrate cannot contain B. Considering that the titanium content in the substrate is negligible, it can be stated that the coating contains predominantly Ti and B with a ratio of (1:6) and the presence of oxygen. Consequently, the boron content in the resulting coating is about 80 at. %.

Table 2.
Elemental composition of the sample in the areas with and without coating.

Point of measurement	Elemental composition, at.%			
	Fe	B	C	O
1	29.0	25.6	16.9	13.6
2	53.3	2.9	24.3	0.2
	Cr	Ti	Ni	Si
1	7.8	4.3	2.3	0.5
2	13.3	0.1	5.6	0.3

The diffraction pattern of the sample is shown in Figure 2.

The studied sample has a polycrystalline structure with a high degree of texture and crystallinity. The most intensive diffraction peaks are characteristic of the phase of the austenitic steel (PDF # 00-033-0397), which was used as a substrate for sputtering. A detailed analysis of the diffraction peaks showed that the peaks at 2θ = (50-51)^{o} and 2θ = (64-65)^{o} have a broadening in the region

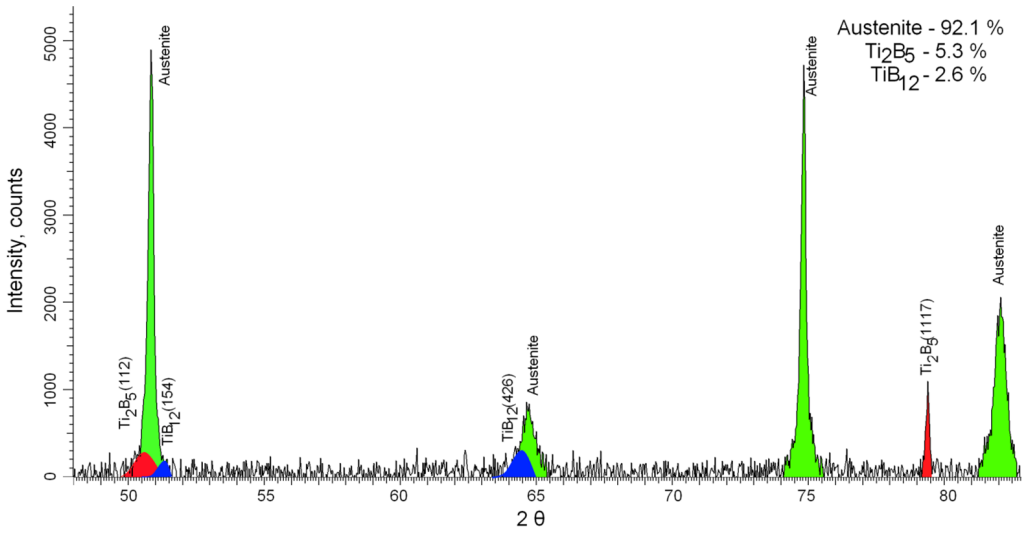

Figure 2. Diffractogram of the studied sample.

of large angles and additional low-intensity maxima, the presence of which may be due to the presence of additional phases characteristic of the deposited layer of titanium boride. Using the obtained diffractograms and the Rietveld method, the phase composition of the sample coating was determined. According to the obtained data, the coating is characterized by a mixture of two phases: the hexagonal phase of Ti_2B_5 with spatial syngony P(0), and the orthorhombic phase TiB_{12} with spatial syngony Imma (74). The volume fraction of the contribution of phases characteristic for titanium boride was determined using the equation (1):

$$V_{admixture} = \frac{RI_{phase}}{I_{admixture+RI_{admixture}}}, \quad (1)$$

I_{phase} is the average integral intensity of the main phase of the diffraction line, Iadmixture is the average integrated intensity of the additional phase, and R is the structural coefficient equal to 1.45. According to the data obtained, the contribution of the phases characteristic of the deposited layer is 7.9%. In this case, it is necessary to take into account the fact that the deposited layer is (5-7)% of the total studied volume. An analysis of the phase content without account for the substrate showed the following ratio of the phase content: 66.8% for the Ti_2B_5 phase and 33.2% for the TiB_{12} phase.

Analyzing the width and area of the line of diffraction maxima, one can estimate the contribution of various defects to the change in the properties of the material. Moreover, an increase in the widths of diffraction lines can be due to micro strains in the structure, which are associated with the accumulation of dislocations, as well as crushing of crystallites caused by crystallization processes. An analysis of the angular dependence of physical broadening makes it possible to estimate the influence of both factors. To assess the impact, the Williamson-Hall method, based on the relation (2), was used:

$$\beta^2 = W_{size}^2 + W_{strain}^2, \quad (2)$$

$$W_{size}^2 = \left(\frac{\lambda}{D \cdot cos(\theta)}\right)^2, \tag{3}$$

$$W_{strain}^2 = (4 \cdot \epsilon \cdot tan(\theta))^2, \tag{4}$$

where β is the physical broadening of the diffraction maximum, λ is the X-ray wavelength (1.54 Å), D is the crystallite size, θ is the Bragg diffraction angle, and ε is the value of the micro strains in the lattice. According to the data obtained, the main contribution to the broadening and change in the form of the diffraction maxima is caused by micro strains arising during crystallization in the process of coatingsynthesis. Micro strains were estimated from the analysis of the displacement of the diffraction peaks calculated according to the equation (3):

$$microstrain = \frac{d_{exp} - d_0}{d_0}, \tag{5}$$

where d_{exp} is the experimentally measured interplanar distance, d_0 is the reference value, which can be found in the PDF 2 database.

The coefficient of the structure deformation was calculated using the equation (4):

$$\varepsilon = \left|\frac{a_0 - a}{a_0}\right|, \tag{6}$$

where a_0 and a are the reference and experimentally obtained values of the unit cell parameter.

The change in the parameters of the crystal lattice caused by the resulting distortions and deformation in the structure, leads to a change in the volume of the crystal lattice and, consequently, the density of the material. The density of the material was calculated using the formula (5):

$$p = \frac{1.6602 \sum AZ}{V_0}, \tag{7}$$

where is the volume of the unit cell, Z is the number of atoms in the crystalline cell, and A is the atomic weight of the atoms. The integral porosity of the studied samples was found according to the formula (6):

$$P_{dil} = (1 - p/p_0) \cdot 100\%, \tag{8}$$

where p_0 is the density of the reference sample.

Table 3 shows changes in the main crystallographic characteristics of the studied sample.

From the ratio of the elements of the main phase it follows that the content of boron in the coating is $\approx 80\%$.

The absence of the phase containing oxygen and carbon gives grounds to suppose that it is in an unbound state. Probably, its presence plays a role in the formation of lattice defects.

Table 3.
Data of crystallographic characteristics.

Phase	Crystal lattice parameters, Å	Micro strains, %		Coefficient of lattice deformation	Density, g/cm^3	Integral porasity, %
Ti2B5	aexp=3.63215	(112)	0.036	0.0012	3.971	0.75
Ti2B5	cexp=27.41830	(1117)	0.16	0.0012	3.971	0.75
TiB12	aexp=12.55430	(154)	0.142	0.01	2.703	1.27
TiB12	bexp=12.81759	(426)	0.069	0.01	2.703	1.27
TiB12	cexp=10.16583	(426)	0.069	0.01	2.703	1.27

The results of investigations of the structure and composition of the synthesized coating showed that the phase composition of the coatings obtained by magnetron sputtering is a mixture of phases consisting of 66.8% of Ti_2B_5 and 33.2% of TiB_{12}. The total concentration of boron atoms in the coating is up to $\approx$80%. This is significantly higher than the boron concentration in the coatings synthesized by other widely used methods, for example, such as plasma technologies.

Conclusion

The carried out experiment on the synthesis of the coating with the B-Ti system shows a sufficient efficiency of using a cathode target of a complex composition, which determines the prospects of the chosen technique.

Investigations of the structure and elemental composition of neutron-absorbing coatings based on titanium boride showed that magnetron sputtering of a complex B_4C-Ti target makes it possible to obtain titanium boride compounds consisting of two phases: Ti_2B_5 and TiB_{12}. This enables us to achieve a boron concentration in the coating $\approx$4 times higher than that obtained in the plasma deposition of the B_4C powder and provides a rather uniform distribution of the elements.

Deposition for 30 minutes allowed to synthesis coating with thickness of 370 nm, but low coating thickness does not allow to obtain sufficiently accurate data on structure and phase composition and determine the role of O and C in the formation of the coating structure. The next step is to create a coating under the same conditions with a thickness of at least 1 μm.

Acknowledgments

This work was supported by the grant AP05134758MOS RK.

References

[1] N.S. Tsebakovskaya et al., Survey of Foreign Practices of SNF and RW Disposal (Komtehprint, Moscow, 2015) 208 p.
[2] Licensing Requirements for the Independent Storage of Spent Nuclear Fuel, High-Level Radioactive Waste and Reactor-Related Greater Than Class C Waste. 10 CFR Part 72 – 2006 Energy.
[3] J.S. Choi et al., Applications of Neutron-Absorbing Structural-Amorphous Metal (SAM) Coatings for Criticality Safety Controls of Used Fuel Storage, Transportation, and Disposal. ICNC 2015 Charlotte, NC, United States September 13-17, 2015.
[4] J-S. Choi et al., Materials Science & Technology 2007 Conference and Exhibition Detroit, MI, United States (2007).
[5] J. Choi et al., 2006 MRS Fall Meeting Boston, MA (2006) UCRL-CONF-226122.
[6] C.M.T. Sanchez et al., Surface & Coatings Technology **205** (2011) 3698.
[7]S.V. Denbnovetsky, Technology and design in electronic equipment **6** (2002).
[8] N.S. Boltovets et al., Tech. Phys. **48**(4) (2003) 441.